

The derivation of the green vegetation fraction from NOAA/AVHRR data for use in numerical weather prediction models

G. GUTMAN and A. IGNATOV

NOAA/NESDIS, Office of Research and Applications, World Weather Building, Washington, DC 20233, USA

(Received 1 July 1997; in final form 2 October 1997)

Abstract. Fraction of green vegetation, f_g , and green leaf area index, L_g , are needed as a regular space-time gridded input to evapotranspiration schemes in the two National Weather Service (NWS) numerical prediction models—regional Eta and global medium range forecast. This study explores the potential of deriving these two variables from the NOAA Advanced Very High Resolution Radiometer (AVHRR) normalized difference vegetation index (NDVI) data. Obviously, one NDVI measurement does not allow simultaneous derivation of both vegetation variables. Simple models of a satellite pixel are used to illustrate the ambiguity resulting from a combination of the unknown horizontal (f_g) and vertical (L_g) densities. We argue that for NOAA AVHRR data sets based on observations with a spatial resolution of a few kilometres the most appropriate way to resolve this ambiguity is to assume that the vegetated part of a pixel is covered by dense vegetation (i.e., its leaf area index is high), and to calculate $f_g = (\text{NDVI} - \text{NDVI}_0) / (\text{NDVI}_\infty - \text{NDVI}_0)$, where NDVI_0 (bare soil) and NDVI_∞ (dense vegetation) are specified as global constants independent of vegetation/soil type. Global $(0\text{--}15^\circ)^2$ spatial resolution monthly maps of f_g were produced from a 5-year NDVI climatology and incorporated in the NWS models. As a result, the model surface fluxes were improved.

1. Introduction

Modern land surface parameterizations (LSP) in numerical weather prediction and general circulation models require specification of two major vegetation characteristics—vegetation type and amount (see review by Avissar and Verstraete 1990). Vegetation type is usually prescribed from the available global vegetation maps based on ground observations (e.g., Matthews 1995). Vegetation amount is parameterized through the fractional area of the vegetation occupying each model grid cell (horizontal density) and the leaf area index, i.e., the number of leaf layers of the vegetated part (vertical density).

The evapotranspiration (as well as photosynthesis) is controlled by green vegetation fraction, f_g , and green leaf area index, L_g . Improved LSPs are being tested in the operational regional (Eta) and global medium range forecast (MRF) models at the National Centers for Environmental Prediction (NCEP) of the National Weather Service (NWS) (Chen *et al.* 1996, H.-L. Pan, personal communication). These LSPs calculate evaporation as a weighted average, with f_g as the weighting factor, of the evaporation from soil and the evapotranspiration from vegetation, the latter being dependent on the number of vegetation layers, L_g . Numerical models, that used modern LSPs, have shown sensitivity of the predicted fluxes to f_g (Jacquemin and Noilhan 1990) and L_g (Chase *et al.* 1996). However, global/seasonal

distributions of these vegetation variables are unknown, so that rather arbitrary tabulated values have often been used based on ground observations over different vegetation types (Chen *et al.* 1996, Viterbo and Beljars 1995). The only way to specify f_g and L_g for large areas, e.g., for the USA in the Eta model or for the globe in the MRF model, is from satellite, and that was the motivation of the present study.

Global data sets containing information on land surface characteristics have been produced from the Advanced Very High Resolution Radiometer (AVHRR) onboard NOAA satellites (see reviews in Townshend 1994, Gutman 1994, Prince and Goward 1996). Among various AVHRR-derived vegetation indices (Huete *et al.* 1994), the most frequently used for global applications is the normalized difference vegetation index (NDVI) = $(\rho_2 - \rho_1)/(\rho_2 + \rho_1)$, where ρ_1 and ρ_2 are reflectance measurements in AVHRR channels 1 (0.63 μm) and 2 (0.85 μm). The use of vegetation indices presently remains the only practical approach to global analysis of AVHRR multi-temporal data on vegetation owing to partial cancellation of the bi-directional, atmospheric and other interfering effects in satellite radiances.

The main goal of the current work was to explore the potential of deriving the above vegetation variables from NDVI for use in numerical models, specifically for the two NCEP models. A simple procedure was analysed and used to derive global $(0.15^\circ)^2$ spatial resolution monthly f_g maps from the global AVHRR NDVI data.

2. Sub-pixel variability and modelling at-sensor signal

The same NDVI signal may result from different sub-pixel structures of a satellite pixel (Price 1992). Figure 1 shows possible combinations of horizontal and vertical densities and their respective models, which are discussed below.

2.1. Uniform-pixel model

Some authors consider pixels fully covered by green vegetation ($f_g = 1$) with a certain vertical density (figure 1, bottom). In this case the signal, attenuated by L_g layers of vegetation, is often presented based on a modified Beer's law (Baret and Guyot 1991, Kustas *et al.* 1993a, Choudhury *et al.* 1994, Sellers *et al.* 1996):

$$\text{NDVI} = \text{NDVI}_\infty - (\text{NDVI}_\infty - \text{NDVI}_0) \exp(-kL_g) \tag{1}$$

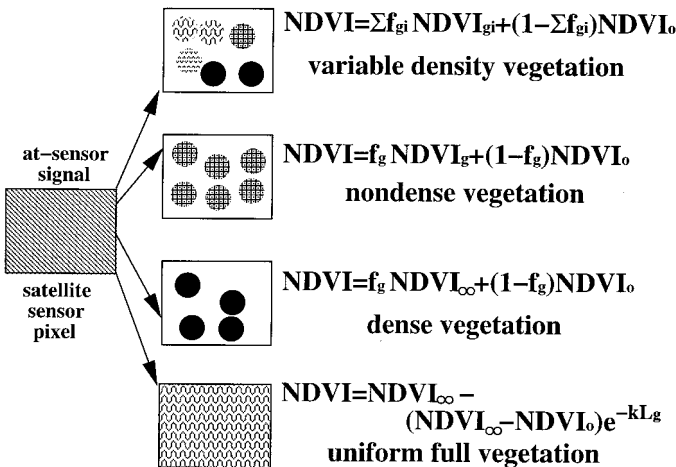


Figure 1. Schematic representation of satellite sensor pixel models.

where NDVI_0 and NDVI_∞ , are the signals from bare soil ($L_g \rightarrow 0$) and dense green vegetation ($L_g \rightarrow \infty$) respectively, and k is the extinction coefficient. Note that the derivation of L_g requires knowledge of three constants: NDVI_0 , NDVI_∞ , and k , the latter characterizing the vegetation type (e.g., Choudhury *et al.* 1994).

2.2. Mosaic-pixel models

Other investigators assume that a pixel has a 'patchy' (mosaic) structure (Kerr *et al.* 1992, Gillies and Carlson 1995, Wittich and Hansing 1995, Valor and Caselles 1996). Three possible cases are illustrated by the three upper panels of figure 1.

In the case of *dense vegetation* (figure 1, second panel from the bottom), an assumption is made that the density of the vegetated part of the pixel is very high ($L_g \rightarrow \infty$, with $\text{NDVI} \rightarrow \text{NDVI}_\infty$) so that

$$\text{NDVI} = f_g \text{NDVI}_\infty + (1 - f_g) \text{NDVI}_0 \quad (2)$$

Since k does not appear in this formulation, the number of constants needed to determine f_g is two instead of three as in the uniform-pixel model.

In the case of *non-dense vegetation* (figure 1, third panel from the bottom), i.e., $L_g \ll \infty$, a combination of equations (1) and (2) yields:

$$\text{NDVI} = f_g \text{NDVI}_g + (1 - f_g) \text{NDVI}_0 \quad (3)$$

where $\text{NDVI}_g = \text{NDVI}_\infty (\text{NDVI}_\infty - \text{NDVI}_0) \exp(-kL_g)$. Here, the variable L_g has a meaning different from the conventional definition of the green leaf area index, which is 'the area of green leaves per unit area of ground' (e.g., Curran 1983, Price 1992). In contrast, we define L_g as a number of leaf layers over the *vegetated part* of the pixel, referred to as a 'clump' leaf area index by Choudhury *et al.* (1994). L_g can never be < 1 in the mosaic-pixel formulations, whereas the 'effective' leaf area index ($f_g L_g$) may be $< L_g$. For example, if the vegetated part covers only one half of the pixel ($f_g = 0.5$) and contains only one vegetation layer ($L_g = 1$), then the effective leaf area index of the pixel is $(f_g L_g) = 0.5$. In reality, there may exist several vegetation types within a pixel, and their vertical densities may vary, so that the observed NDVI is a weighted average of the NDVIs from different vegetated 'tiles' of the vegetated (NDVI_{gi}) and non-vegetated (NDVI_0) parts (figure 1, top): $\text{NDVI} = \sum f_{gi} \text{NDVI}_{gi} + (1 - \sum f_{gi}) \text{NDVI}_0$, where $\text{NDVI}_{gi} = \text{NDVI}_\infty - (\text{NDVI}_\infty - \text{NDVI}_0) \exp(-k_i L_{gi})$ and the summation is over all the vegetated 'tiles' within the pixel with the corresponding fractions f_{gi} .

2.3. Choosing an appropriate pixel model for AVHRR

The choice between the uniform- and mosaic-pixel models would depend upon spatial resolution of satellite sensor data and the structure of vegetation, the latter being geographic region- and vegetation type-specific. In processing global data, it is difficult to identify and adjust the retrieval model, and therefore simplified approaches are often used. For example, Sellers *et al.* (1996) and Nemani *et al.* (1996) derived L_g assuming $f_g = 1$ for each satellite sensor pixel. It is plausible to assume that a pixel is more uniform or mosaic as the spatial resolution increases or degrades, respectively (Price 1992). For AVHRR global data sets, produced from observations with a spatial resolution of a few kilometres, derivation of f_g keeping L_g prescribed and using the *variable density* model seems most appropriate. However, derivation of several unknowns (subpixel values) from just one measurement is infeasible (note that temporal analysis could be used to tackle this problem in local studies

(e.g., Fischer 1994)). The two-parametric *non-dense vegetation* model provides a reasonable trade-off, describing the process simply yet realistically. Recall that the NCEP's models use this same two-parametric description of vegetation in even larger model grid cells (30–100 km), which makes us more confident of its validity on AVHRR pixel scales which are typically an order of magnitude less. The problem of deriving two unknowns— f_g and L_g —from one NDVI measurement is still ambiguous and requires an additional constraint. Using two reflectances and/or their combination with thermal IR data could potentially resolve that ambiguity (e.g., Jasinski 1990, Carlson *et al.* 1990, Hanan *et al.* 1991, Price 1992, 1993, Choudhury *et al.* 1994, Gillies and Carlson 1995, Valor and Caselles 1996). However, these methods are applicable only to studies for restricted space-time scales, when atmosphere and sun-view geometry are either non-variable or can be corrected for. This is not considered in the present study, which is directed at global applications.

2.4. *Resolving the ambiguity: the dense vegetation model*

Figure 2 shows that the NDVI, calculated from equation (3) as a function of f_g and L_g , is their unresolved combination. This implies that one NDVI measurement does not allow simultaneous derivation of f_g and L_g . This complexity, discussed by Price (1992, 1993), can be compared to remote sensing of clouds when the satellite signal is a combined effect of horizontal (fractional cover, analogue of f_g) and vertical (cloud optical thickness, analogue of kL_g) densities. One way to resolve this ambiguity is to assume that these two variables are coupled, as it was done in the pioneering Deardorff's (1976) LSP. An assumption of a coherent seasonal cycle in the vertical and horizontal vegetation densities seems reasonable. Yet, no sufficient basis exists for reliable relationships, which are expected to be site- and morphology-specific.

Alternatively, one can prescribe one of the two variables and derive the second. Equation (1) and figure 2 provide additional rationale why one would rather

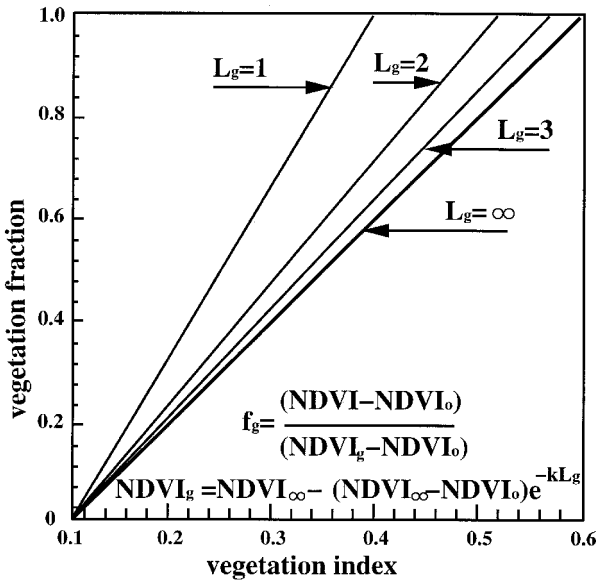


Figure 2. Fraction of green vegetation as a function of NDVI and leaf area index. The mosaic non-dense vegetation model is also shown.

prescribe L_g , and derive f_g : the exponential dependence $\text{NDVI}(L_g)$ ‘saturates’ after a certain threshold, L_g^{sat} , and NDVI becomes insensitive to L_g . The saturation threshold, L_g^{sat} , depends on the vegetation type, characterized by the extinction coefficient, k . Carlson *et al.* (1990) reported that for ground observations $2 < L_g^{\text{sat}} < 6$. This circumstance is unfortunate for the L_g estimate but favourable for the f_g estimate, since the function $f_g(\text{NDVI})$ in figure 2 is strong and almost unambiguous for $L_g > L_g^{\text{sat}}$. By prescribing f_g , the value of L_g can be potentially derived when $1 < L_g < L_g^{\text{sat}}$. But even then, the derivation of L_g requires the coefficient k , which itself is uncertain. The derivation of f_g from NDVI data is, thus, better founded and should be more accurate than L_g .

To derive f_g , a value of $L_g \geq 1$ has to be prescribed. For the present study, we have chosen $L_g = \infty$. In practice, this means that L_g is high enough to allow neglecting the exponent term in equation (1): $\exp(-kL_g) = 0$. Figure 2 shows that for $k = 1$ the exponent term becomes negligible when $L_g > 3$. As a result, the formulation reduces to the *dense vegetation* model.

3. Results

3.1. Global production of f_g maps

The values of NDVI_0 and NDVI_∞ , needed for deriving f_g from equation (2) should be region- and season-specific, since they depend on the soil and vegetation types and the vegetation chlorophyll content (e.g., Price 1992, Huete *et al.* 1994), hence they are to be derived from the data (e.g., Kerr *et al.* 1992). They can be estimated as minimum and maximum NDVI , NDVI_{min} and NDVI_{max} , in each space-time box, assuming one can find bare-soil and fully vegetated pixels within each box. Sellers *et al.* (1996), for example, defined NDVI_0 and NDVI_∞ , as the lower and upper 2–5% NDVI for each biome.

The following exercise illustrates our attempt to apply this idea to GVI data. Figure 3 shows the results of a cluster analysis of about 650 000 points from GVI $(0.15^\circ)^2$ annual data using annual minimum NDVI_{min} , and maximum, NDVI_{max} , as the clustering variables in the nearest centroid sorting method (SAS 1989). (Analysis shows that the results are insensitive to the number of clusters—in this example, seven were used.) In the areas with highly seasonal vegetation, there is a good chance that during the course of the year we can observe bare soil pixels and those that are fully covered with dense vegetation. This means that both NDVI_0 and NDVI_∞ , may

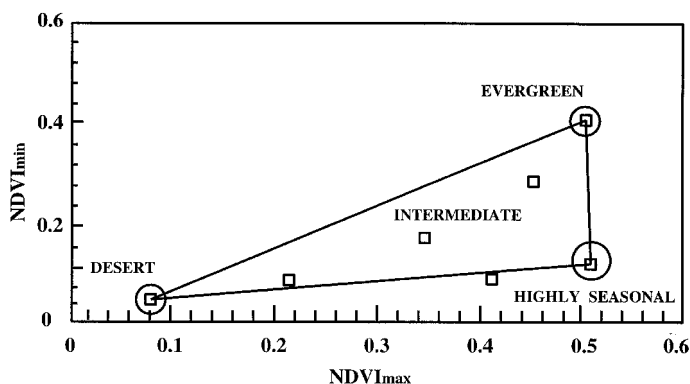


Figure 3. The ‘global triangle’ of surface types: the results of cluster analysis using NDVI ’s annual maximum and minimum.

be reliably derived from data itself over those areas. In some areas, such as deserts and evergreen vegetation, either bare soil or fully vegetated pixels are observed throughout the year, respectively. In both cases, only one of the two constants ($NDVI_0$ and $NDVI_\infty$) can be reliably derived. The three major clusters are shown as the corners of a global triangle' in figure 3 (cf. with DeFries and Townshend 1994), with the radii representing RMS standard deviation for the clusters. Figure 4 shows a global view of the spatial distribution of these clusters using a red-green composite, with red as the annual range $NDVI_{max} - NDVI_{min}$ and green as the annual maximum $NDVI_{max}$. (This representation of surface types is similar to earlier works by Tucker *et al.* (1985) and Townshend *et al.* (1985).) Figures 3 and 4 show that there are many intermediate cases, in which it may be difficult to find the bare soil or fully vegetated pixels for regional adjustment of $NDVI_0$ and $NDVI_\infty$ (cf. with Valor and Caselles 1996). Therefore, we prescribe $NDVI_0 = 0.04$ (with $\sigma_0 \approx 0.03$) and $NDVI_\infty = 0.52$ (with $\sigma_\infty \approx 0.03$) as seasonally- and geographically invariant constants, which correspond to the $NDVI_{min}$ and $NDVI_{max}$ of the desert and evergreen clusters, respectively. Monthly maps of f_g (figure 5) are then produced from the 5-year NDVI

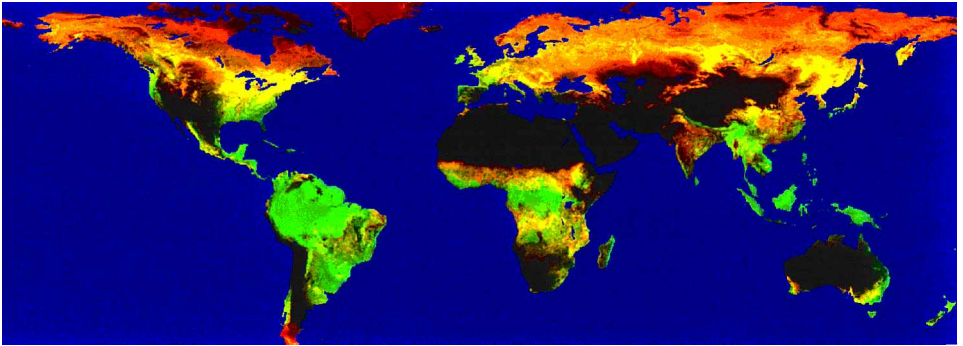


Figure 4. A red-green composite of NDVI's annual range (red) and maximum (green). The major clusters are bright green (evergreen), bright yellow (highly seasonal), and dark brown (desert). The areas with scarce vegetation that are covered by snow during winter are rendered in reddish colours.

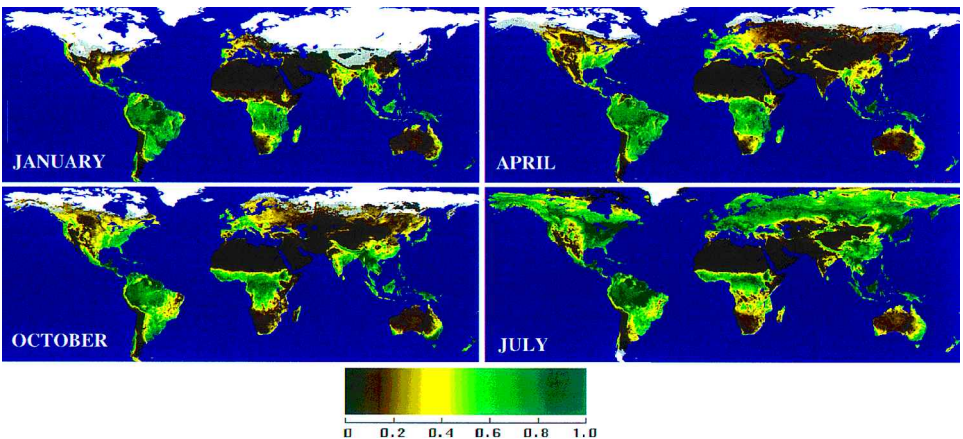


Figure 5. Seasonal cycle of fractional vegetation. The snow mask is described in Gutman *et al.* (1995).

climatology (Gutman *et al.* 1995) with a $(0.15^\circ)^2$ spatial resolution using the *dense vegetation mosaic-pixel* model (equation 2) resolved for f_g , which was restricted to 0–1 interval:

$$f_g = (\text{NDVI} - \text{NDVI}_o) / (\text{NDVI}_\infty - \text{NDVI}_o) \quad (4)$$

3.2. Error analysis

3.2.1. The f_g —NDVI linearity

The validity of the linear relationship (2) has been confirmed by Ormsby *et al.* (1987), Carlson *et al.* (1990), Phulpin *et al.* (1990), Myneni *et al.* (1992), Kustas *et al.* (1993b), and Wittich and Hansing (1995). According to these studies, the non-linearity of the relationship $f_g(\text{NDVI})$ was beyond the detectability over a wide range of vegetation densities. Wittich and Hansing (1995) estimate that the residual error of the linear regression does not exceed $\sigma \approx 0.1$, which represents the worst case error in f_g , associated with the use of equation (2).

3.2.2. The dense vegetation assumption

Myneni *et al.* (1992) pointed out that the slope of this linear relationship depends on L_g . This conclusion is in agreement with figure 2 which shows that the error in f_g resulting from the ‘dense vegetation’ assumption is negligible when $f_g \rightarrow 0$ and gradually increases with f_g . However, even for $f_g \rightarrow 1$, the error is $\sigma < 0.1$ when $L_g > 3$. The greatest errors may occur when $1 < L_g < 3$ over areas with $\text{NDVI} \approx 0.25$ – 0.50 —presumably at the beginning and end of the growing season. In contrast, the most reliable results on f_g are expected at the peak of the growing season, when L_g is at its maximum, and before the growing season, when NDVI is small.

3.2.3. Variability in NDVI_o and NDVI_∞

It is known that there is an impact of soil reflectance on the relationship between f_g and NDVI, through the variable NDVI_o in equation (2) (e.g., Jasinski 1990, Minessy *et al.* 1992, Huete *et al.* 1994). On the other hand, NDVI_∞ (saturation greenness) is expected to depend upon the type, geometric structure, and chlorophyll content and physiology (mesophyll) of vegetation (Curran 1983, Carlson *et al.* 1990). Additionally, NDVI depends upon atmospheric conditions and sun-view geometry of observations. Assuming that all these factors result in random errors in NDVI_o and NDVI_∞ , σ_o and σ_∞ , the RMS error of the f_g estimate is:

$$\sigma = \{ [f_g \sigma_\infty]^2 + [(1 - f_g) \sigma_o]^2 \}^{1/2} / (\text{NDVI}_\infty - \text{NDVI}_o) \quad (5)$$

For $f_g \rightarrow 0$ and $f_g \rightarrow 1$, the worst case error 3σ is about 0.18, and for $f_g = 0.5$, it is ≈ 0.12 .

3.2.4. The total error

Summarizing, the worst case error might amount to about 0.35, which implies a reliable distinction of three gradations. In general, we can expect more than three gradations for f_g owing to errors smaller than those estimated above and their partial compensation. Note that the derived f_g is also influenced by the imperfection of the NDVI data: errors from residual cloud contamination and atmospheric/angular/shadowing effects. These effects, compounded with the seasonal cycle and global variability in illumination conditions, introduce systematic biases since NDVI_∞ and NDVI_o are constant. For example, tropical forests, where f_g is expected to be 1, are often the areas of persistent clouds, and, as result, the value of f_g may

be somewhat underestimated. All of the above dictates the necessity for improving the NDVI data to minimize the above biases that directly propagate into the f_g data set.

3.3. *The relative merit of the satellite-derived f_g product*

Despite the above uncertainties, the f_g satellite product is deemed to be a realistic specification of the seasonal global vegetation cover distribution that fits the current requirements of NCEP LSPs. Its validation for the globe is difficult, if feasible at all, as with many other land surface products, but that is not the major issue. Of greater relevance here is the consistency of the derived product with the simplified description of complicated air-surface interactions in present LSPs. Note that both f_g and L_g are merely effective model variables that could yield good results in a model and still disagree with conventional data on those variables. The measure that quantifies the effect of the incorporation of regional seasonal changes in vegetation cover is the model surface fluxes and the proportion of the latent and sensible heat fluxes in the heat balance. The ultimate criterion of the merit of any input in an LSP is, of course, improvement of the weather forecast. Presently, the monthly maps of green vegetation fraction have been incorporated in NCEP models and the preliminary results are encouraging. Betts *et al.* (1997) used Eta model 3-D reruns to show that the use of the present f_g data produce model surface fluxes closer to the observations. More sensitivity studies are planned to assess the impact of the uncertainties in satellite sensor data on the model fluxes. Unfortunately, testing the impact of the newly incorporated f_g is hindered by the prohibitive expenses of operational model runs.

4. Conclusion

The main goal of the current work was to produce monthly data of green vegetation fraction, f_g , for use in numerical models, specifically for NCEP forecast models. A simple procedure was analysed and used to derive global $(0.15^\circ)^2$ spatial resolution monthly f_g maps from the NOAA GVI data set. We showed that the problem of f_g estimation from AVHRR data is underdetermined and proposed to use a dense vegetation assumption to resolve the ambiguity. Preliminary results on incorporation of the vegetation fraction maps in NWS numerical weather prediction models show an improvement of the predicted surface fluxes. Our data specify a more realistic and consistent model input than the previously prescribed spatially and temporally invariant vegetation fraction. In considering the currently available satellite-derived global fields of f_g (the present study) and L_g (Sellers *et al.* 1996, Nemani *et al.* 1996), one must bear in mind that both are obtained from one variable—NDVI—and are nothing more than two different ways to interpret the same satellite sensor data. Therefore, they cannot be regarded as two independent pieces of information on the vegetation cover and should not be used in tandem within the same LSP. With present AVHRR data, either independently prescribed L_g or established f_g — L_g relationships are recommended as pragmatic steps forward. Using data from other sensors with high spatial resolution would allow application of the uniform-pixel model to derive L_g assuming $f_g = 1$, with further aggregation of high spatial resolution satellite retrievals into model-size grid cells (≈ 30 – 100 km). The required spatial resolution of satellite sensor data has to be investigated before recommendations can be given. The key issue remains increasing the quality of satellite data sets with better cloud screening and angular/atmospheric corrections

applied (Prince and Goward 1996). Global data from other sensors with better spectral characteristics and more complete angular sampling should be considered (e.g., Roujean *et al.* 1997, Huete *et al.* 1994).

The f_g data can be accessed using 140.90.197.192 anonymous file transfer protocol (ftp), directory /pub/ggutman/frveg.

Acknowledgement

This work was supported by the NOAA Global and Climate Change Program through the NCEP. We greatly appreciate strong personal support by Drs Ken Mitchell (NCEP) and Dan Tarpley (NESDIS) and fruitful discussions with them and Dr Fei Chen (NCEP/UCAR). Thanks go to Dr George Ohring (NESDIS) and the anonymous reviewers for reviewing the manuscript. This work was done when A.I. was a University Corporation for Atmospheric Research visiting scientist at NOAA/NESDIS on leave from the Marine Hydrophysics Institute, Sevastopol, Ukraine.

References

- AVISSAR, R., and VERSTRAETE, M. M., 1990, The representation of continental surface processes in atmospheric models. *Reviews of Geophysics*, **28**, 35–52.
- BARET, F., and GUYOT, G., 1991, Potential and limits of vegetation indices for LAI and APAR assessment. *Remote Sensing of Environment*, **35**, 161–173.
- BETTS, A. K., CHEN, F., MITCHELL, K. E., and JANJIC, Z. I., 1997, Assessment of the land-surface and boundary-layer models in two operational versions of the NCEP Eta model using FIFE data. *Monthly Weather Review*, **125**, 2896–2916.
- CARLSON, T. N., PERRY, E. M., and SCHMUGGE, T. J., 1990, Remote estimates of soil moisture availability and fractional vegetation cover for agricultural fields. *Agriculture and Forest Meteorology*, **52**, 45–70.
- CHASE, T. N., PIELKE, R. A., KITTEL, T. G. F., NEMANI, R., and RUNNING, S. W., 1996, Sensitivity of a general circulation model to global changes in leaf area index. *Journal of Geophysical Research*, **101**, 7393–7408.
- CHEN, F., MITCHELL, K., SCHAAKE, J., XUE, Y., PAN, H., KOREN, V., DUAN, Q., and BETTS, A., 1996, Modelling of land-surface evaporation by four schemes and comparison with FIFE observations. *Journal of Geophysical Research*, **101**, 7251–7268.
- CHOUDHURY, B. J., AHMED, N. U., IDSO, S. B., REGINATO, R. J., and DAUGHTRY, C. S. T., 1994, Relations between evaporation coefficients and vegetation indices studied by model simulations. *Remote Sensing of Environment*, **50**, 1–17.
- CURRAN, P. J., 1983, Multispectral remote sensing for the estimation of green leaf area index. *Philosophical Transactions of the Royal Society (London)*, **309**, 257–270.
- DEARDORFF, J. W., 1978, Efficient prediction of ground surface temperature and moisture, with inclusion of layer of vegetation. *Journal of Geophysical Research*, **83**, 1889–1903.
- DEFRIES, R. S., and TOWNSHEND, J. R. G., 1994, NDVI-derived land cover classifications at a global scale. *International Journal of Remote Sensing*, **15**, 3567–3586.
- FISCHER, A., 1994, A model for the seasonal variations of vegetation indices in coarse resolution data and its inversion to extract crop parameters. *Remote Sensing of Environment*, **48**, 220–230.
- GILLIES, R. R., and CARLSON, T. N., 1995, Thermal remote sensing of surface soil water content with partial vegetation cover for incorporation into climate models. *Journal of Applied Meteorology*, **34**, 745–756.
- GUTMAN, G. G., 1994, Global data on land surface parameters from NOAA AVHRR for use in numerical climate models. *Journal of Climate*, **7**, 669–680.
- GUTMAN, G., TARPLEY, D., IGNATOV, A., and OLSON, S., 1995, The enhanced NOAA global land data set from the Advanced Very High Resolution Radiometer. *Bulletin of the American Meteorological Society*, **76**, 1141–1156.

- HANAN, N. P., PRINCE, S. D., and HIERNAUX, P. H. Y., 1991, Spectral modelling of multi-component landscapes in the Sahel. *International Journal of Remote Sensing*, **12**, 1243–1258.
- HUETE, A., JUSTICE, C., and LIU, H., 1994, Development of vegetation and soil indices for MODIS–EOS. *Remote Sensing of Environment*, **49**, 224–234.
- JACQUEMIN, B., and NOILHAN, J., 1990, Sensitivity study and validation of a land surface parameterization using the Hapex–Mobilhy data set. *Boundary-Layer Meteorology*, **52**, 93–134.
- JASINSKI, M. F., 1990, Sensitivity of the normalized difference vegetation index to subpixel canopy cover, soil albedo, and pixel scale. *Remote Sensing of Environment*, **32**, 169–187.
- KERR, Y. H., LAGOUARDE, J. P., and IMBERNON, J., 1992, Accurate land surface temperature retrieval from AVHRR data with use of an improved split-window algorithm. *Remote Sensing of Environment*, **41**, 197–209.
- KUSTAS, W. P., DAUGHTRY, C. S. T., and VAN OEVELEN, P. J., 1993a, Analytical treatment of the relationships between soil heat flux/net radiation and vegetation indices. *Remote Sensing of Environment*, **46**, 319–330.
- KUSTAS, W. P., SCHMUGGE, T. J., HUMES, K. S., JACKSON, T. J., PARRY, R., WELTZ, M. A., and MORAN, M. S., 1993b, Relationships between evaporative fraction and remotely sensed vegetation index and microwave brightness temperature for semiarid rangelands. *Journal of Applied Meteorology*, **32**, 1781–1790.
- MATTHEWS, E., 1995, Atlas of archived vegetation, land-use and seasonal albedo data sets. NASA Technical Memo 86199, NASA, Washington, DC.
- MYNENI, R. B., ASRAR, G., TANRE, D., and CHOUDHURY, B. J., 1992, Remote sensing of solar radiation absorbed and reflected by vegetated land surfaces. *I.E.E.E. Transactions on Geosciences Remote Sensing*, **30**, 302–314.
- NEMANI, R. R., RUNNING, S. W., PIELKE, R. A., and CHASE, T. N., 1996, Global vegetation cover changes from coarse resolution satellite data. *Journal of Geophysical Research*, **101**, 7157–7162.
- ORMSBY, J. P., CHOUDHURY, B. J., and OWE, M., 1987, Vegetation spatial variability and its effect on vegetation indices. *International Journal of Remote Sensing*, **8**, 1301–1306.
- PHULPIN, T., NOILHAN, J., and STOLL, M., 1990, Parameters estimates of a soil-vegetation model using AVHRR data. *Proceedings of the 4th AVHRR data users meeting. Rothenburg, Germany, 5–8 September 1989*, EUM P 06 (Darmstadt: EUMETSAT), pp. 125–129.
- PRICE, J., 1992, Estimating vegetation amount from visible and near-infrared reflectances. *Remote Sensing Environment*, **41**, 29–34.
- PRICE, J., 1993, Estimating leaf area index from satellite data. *I.E.E.E. Transactions Geoscience and Remote Sensing*, **31**, 727–734.
- PRINCE, S. D., and GOWARD, S. N., 1996, Evaluation of the NOAA/NASA Pathfinder AVHRR land data set for global primary production modelling. *International Journal of Remote Sensing*, **17**, 217–221.
- ROUJEAN, J. L., TANRE, D., BREON, F. M., and DEUZE, J. L., 1997, Retrieval of land surface parameters from airborne POLDER bi-directional reflectance distribution function during HAPEX–Sahel. *Journal of Geophysical Research*, **102**, 11 201–11 218.
- SAS[SAS INSTITUTE INC.], 1989, *SAS/STAT User's Guide*, Version 6, Fourth Edition, v.1, Cary, North Carolina.
- SELLERS, P. J., LOS, S. O., TUCKER, C. J., JUSTICE, C. O., DAZLICH, D. A., COLLATZ, D. J., and RANDALL, D. A., 1996, A revised land surface parameterization (SiB2) for atmospheric GCMs. Part 2: The generation of global fields of terrestrial biophysical parameters from satellite data. *Journal of Climate*, **9**, 706–737.
- TOWNSHEND, J. R. G., 1994, Global data sets for land applications from the Advanced Very High Resolution Radiometer: an introduction. *International Journal of Remote Sensing*, **15**, 3319–3332.
- TOWNSHEND, J. R. G., JUSTICE, C. O., and KALB, V. T., 1987, Characterization and classification of South American land cover types using satellite data. *International Journal of Remote Sensing*, **35**, 243–256.
- TUCKER, C. J., TOWNSHEND, J. R. G., and GOFF, T. E., 1985, African land-cover classification using satellite data. *Science*, **227**, 369–375.

- VALOR, E., and CASELLES, V., 1996, Mapping land surface emissivity from NDVI: Application to European, African, and South American areas. *Remote Sensing of Environment*, **57**, 167–184.
- VITERBO, P., and BELJARS, A., 1995, An Improved land surface parameterization scheme in the ECMWF model and its validation. *Journal of Climate*, **8**, 2716–2748.
- WITTICH, K. P., and HANSING, O., 1995, Area-averaged vegetative cover fraction estimated from satellite data. *International Journal of Biometeorology*, **38**, 209–215.